

In the format provided by the authors and unedited.

Achromatic metalens array for full-colour light-field imaging

Ren Jie Lin^{1,9}, Vin-Cent Su^{2,9} , Shuming Wang^{3,4,5,9} , Mu Ku Chen^{1,9}, Tsung Lin Chung¹, Yu Han Chen¹ , Hsin Yu Kuo¹, Jia-Wern Chen¹, Ji Chen^{3,4,5}, Yi-Teng Huang¹, Jung-Hsi Wang⁶, Cheng Hung Chu⁷, Pin Chieh Wu⁷, Tao Li^{3,4,5}, Zhenlin Wang^{3,5}, Shining Zhu^{3,4,5*} and Din Ping Tsai^{1,7,8*} 

¹Department of Physics, National Taiwan University, Taipei, Taiwan. ²Department of Electrical Engineering, National United University, Miaoli, Taiwan.

³National Laboratory of Solid State Microstructures, School of Physics, College of Engineering and Applied Sciences, Nanjing University, Nanjing, China.

⁴Key Laboratory of Intelligent Optical Sensing and Manipulation, Ministry of Education, Nanjing, China. ⁵Collaborative Innovation Center of Advanced Microstructures, Nanjing, China. ⁶Department of Electrical Engineering and Graduate Institute of Electronics Engineering, National Taiwan University, Taipei, Taiwan. ⁷Research Center for Applied Sciences, Academia Sinica, Taipei, Taiwan. ⁸College of Engineering, Chang Gung University, Taoyuan, Taiwan.

⁹These authors contributed equally: Ren Jie Lin, Vin-Cent Su, Shuming Wang, Mu Ku Chen. *e-mail: zhushn@nju.edu.cn; dptsai@phys.ntu.edu.tw

Supplementary information

Design and simulation

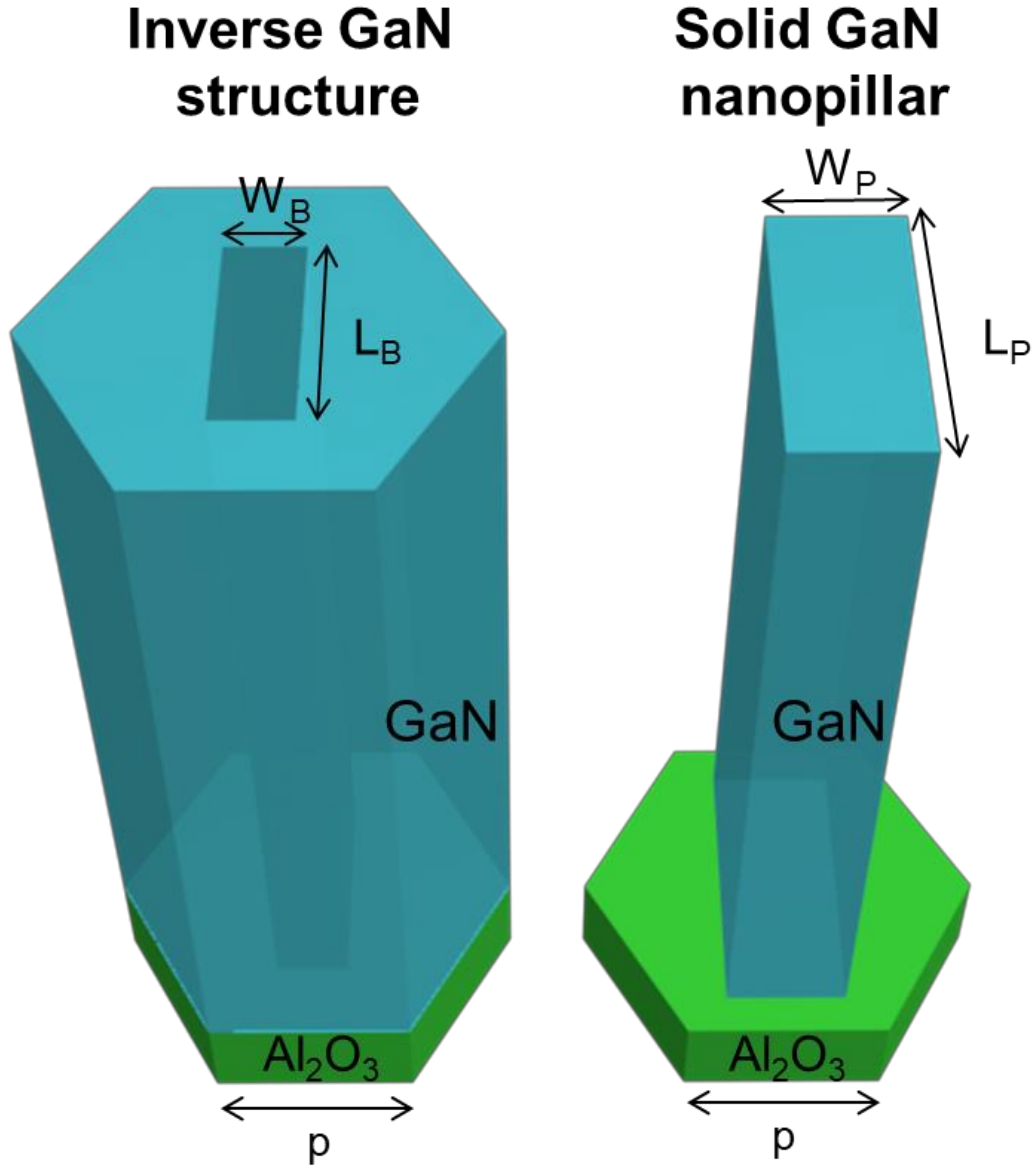
All numerical simulations are carried out using microwave studio commercial software based on the finite integration method from Computer Simulation Technology (CST). GaN nanopillars and inverse structures are chosen as building blocks with high refractive-index and low loss. For the structural optimization of GaN nanostructures, the unit cell boundary condition is utilized by evaluating their transmission spectra and phase shifts. The perfectly matched layer and periodic boundary condition are plotted as the x- and y-directions, respectively, to estimate the focal length of the designed metalens. The refractive index of GaN is obtained from reference 1.

Fabrication

The fabrication processes of the metalens arrays are described as follows. A double-sided polished sapphire substrate oriented along a c-axis [0001] direction is first prepared for the processes. An 800-nm-thick undoped GaN epitaxial layer is subsequently grown on the sapphire substrate by metal-organic chemical vapor deposition (MOCVD). During the growth process, high purity H₂ is used as the carrier gas to transport trimethylgallium (TMGa) and NH₃ to be employed as gallium and nitrogen precursors, respectively.

After the growth of undoped GaN on the sapphire substrate, 400 nm of SiO₂ is deposited as a hard mask layer by using plasma-enhanced chemical vapor deposition (PECVD). Diluted ZEP-520A (ZEP-520A : ZEPA = 1:3), as a positive tone electron-beam resist, is then spin-coated onto the prepared substrate (5000 rpm, 90 seconds) and baked on a hot plate (3 minutes, 180°C) to form a 150-nm resist layer. The achromatic metalens arrays are defined by the exposure of an Elionix ELS-7000 electron-beam lithography system at a 100-kV acceleration voltage with a beam current of 100 pA. The structure profile of the metalens arrays in the exposed substrate is revealed after the development process in ZED-N50 for 5 minutes, followed by rinsing with

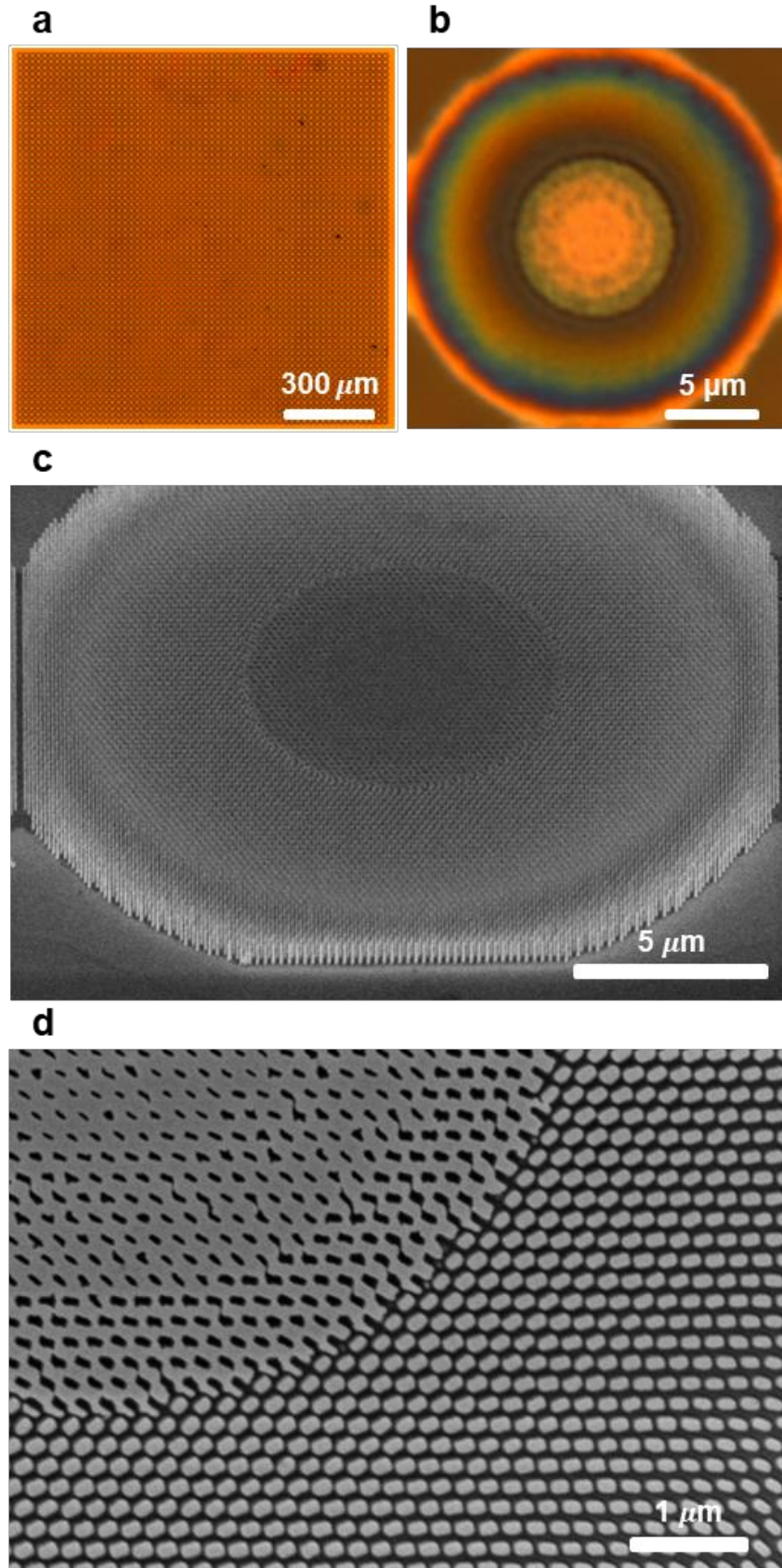
IPA for 10 seconds and drying under a dry N₂ stream. Next, 40 nm of Cr layer is applied by an electron-gun evaporator as a hard etching mask layer . After the lift-off process in a solution of N,N-dimethylacetamide (ZDMAC), the patterns are transferred to the 400-nm-thick SiO₂ hard mask layer by reactive ion etching (RIE) performed at a plasma power of 90 W. Afterwards, an inductively coupled-plasma reactive ion etching (ICP-RIE) system with BCl₃/Cl₂ chemistry is utilized to etch the sample with the patterned SiO₂ hard mask layer. The ICP-RIE system is operated at a radio frequency of 13.56 MHz with an ICP source power of 700 W and a bias power of 280 W. Finally, the sample can be obtained after removing the patterned SiO₂ hard mask by immersion in a buffered oxide etch (BOE) solution.



Supplementary Fig. 1: Schematics of the building blocks of GaN-based achromatic metalenses. Two types of building blocks with a height of 800 nm are used: inverse and solid structures. The lattice constant p is 120 nm. Different combinations of feature sizes, W_B , L_B , W_P and L_P , are considered to satisfy the different phase requirements of achromatic metalenses elaborated in Supplementary Table 1.

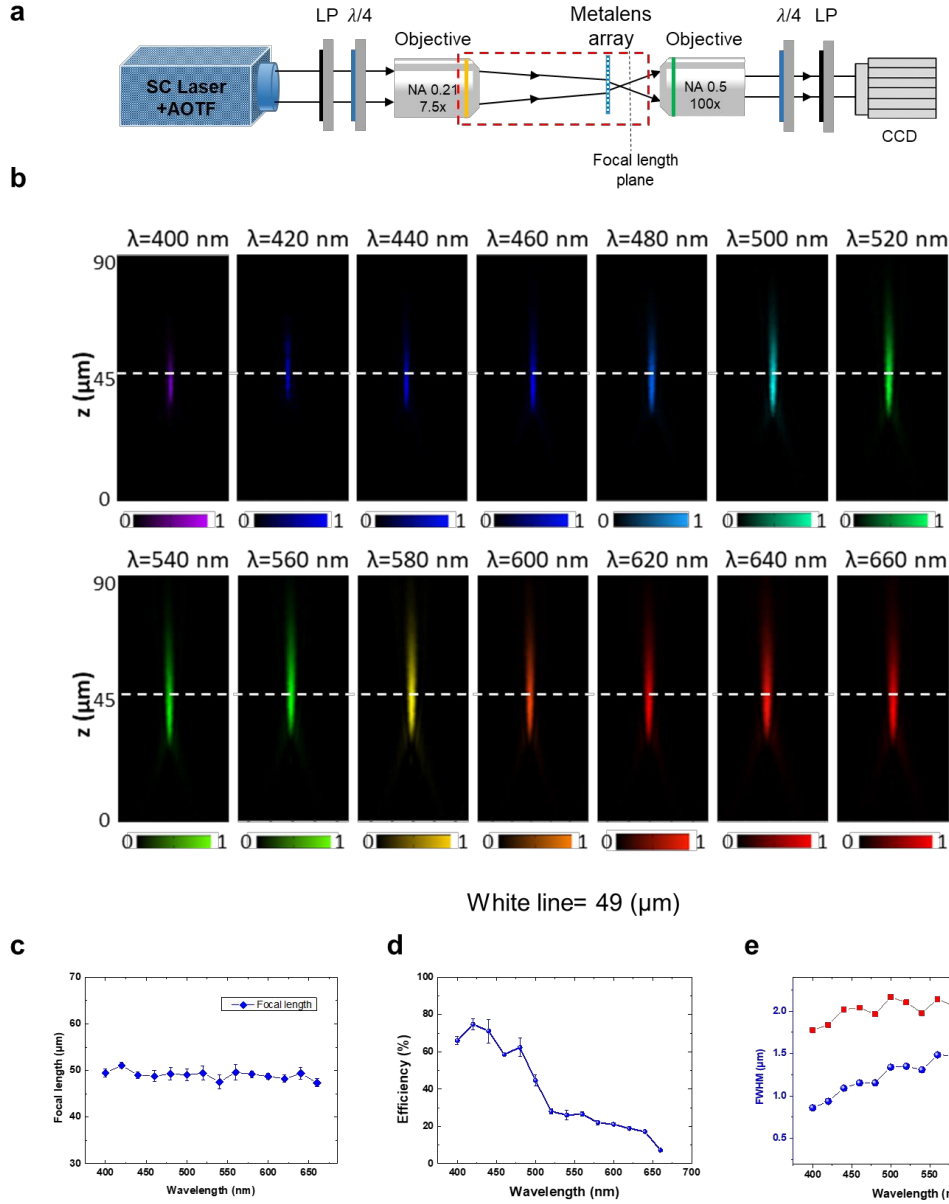
Supplementary Table 1: Feature sizes of GaN nanostructures.

Inverse GaN structures		
L_B (nm)	W_B (nm)	Phase Compensation(°)
125	50	1080
140	60	1110
163	80	1080
Solid GaN nanopillars		
L_P (nm)	W_P (nm)	Phase Compensation(°)
165	110	1050
165	100	1020
155	95	990
150	90	960
145	85	930
140	80	900
140	75	870
135	70	840
135	65	810
130	60	780
125	55	750
115	50	720
95	50	690
80	45	660

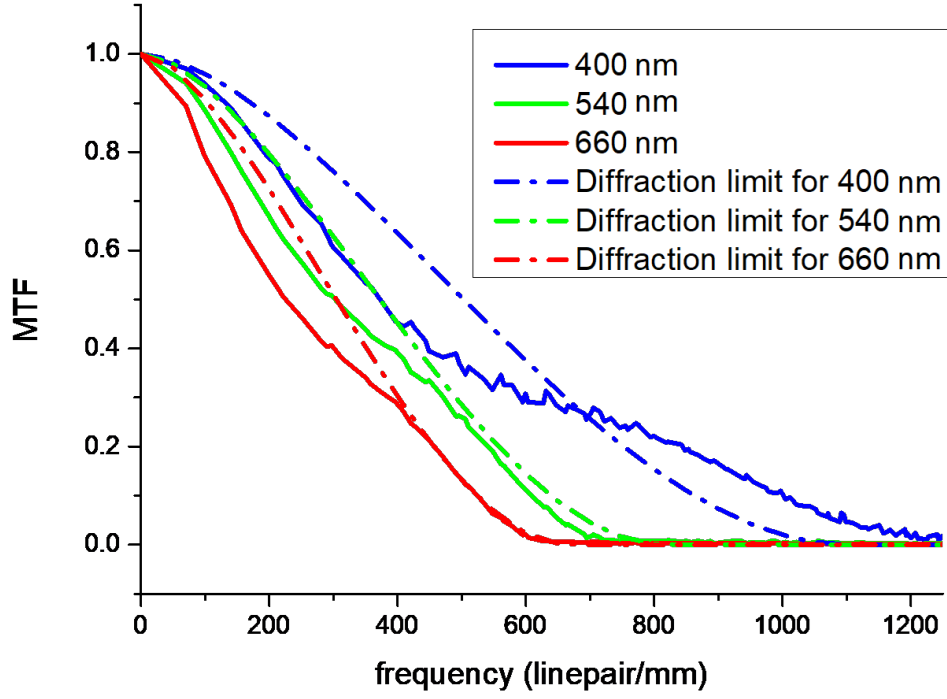


Supplementary Fig. 2: Experimental verification of achromatic metalens array. **a**, Optical image of the fabricated achromatic metalens array with $\text{NA} = 0.2157$. Scale bar: 300 μm . **b**, Optical image of single achromatic metalens. Scale bar: 5 μm . **c**, SEM image of single

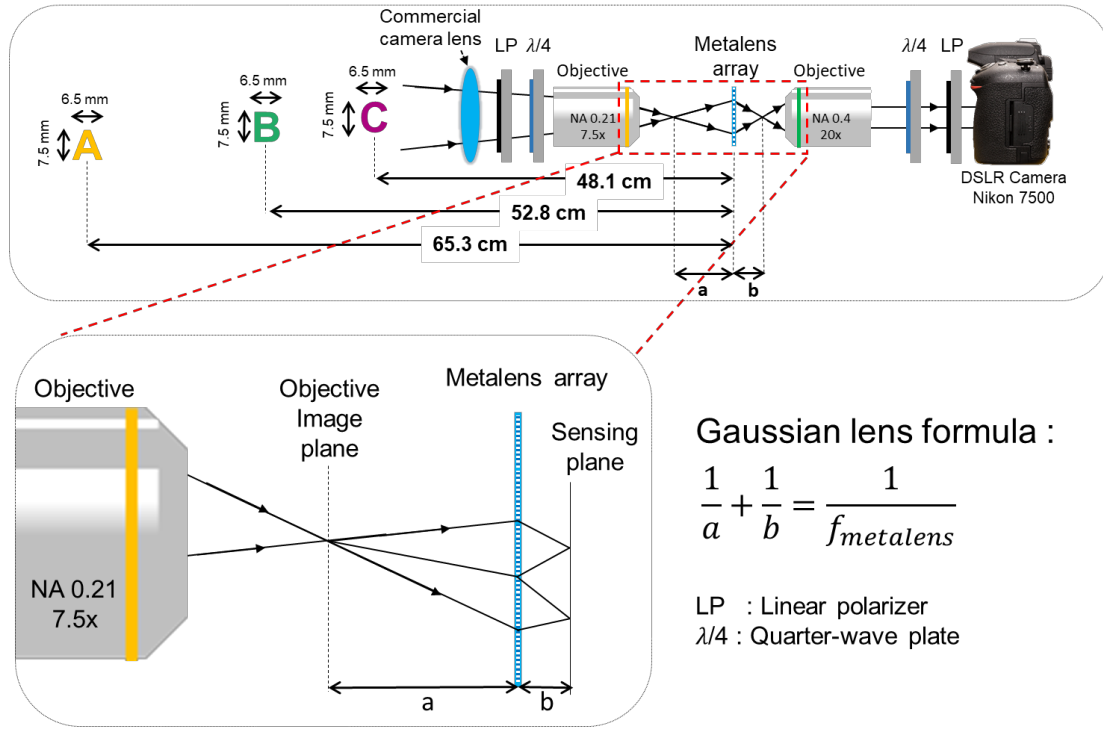
achromatic metalens. Scale bar: $5\mu\text{m}$. **d**, Zoomed-in SEM images at the boundary of nanopillars and inverse GaN-based structures. Scale bar: $1\mu\text{m}$.



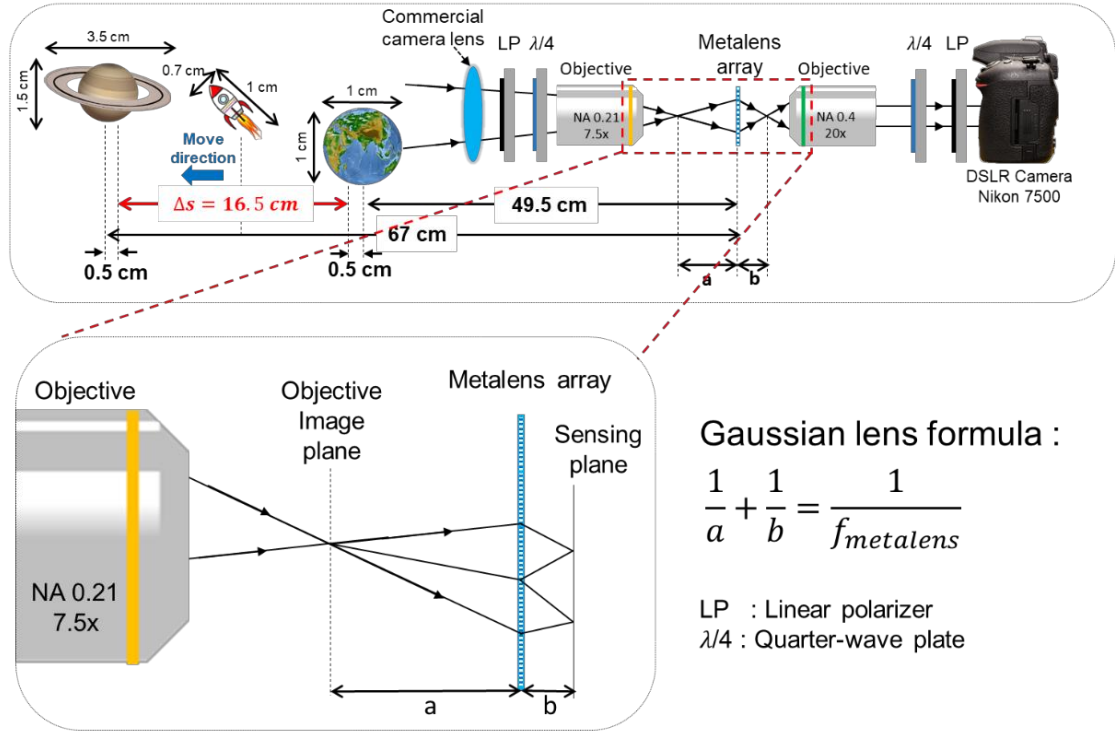
Supplementary Fig. 3: Experimental verification of a single achromatic metalens. **a**, Experimental setup for focusing behavior characterization. **b**, Experimental focusing behavior of achromatic metalens with NA of 0.2157 at various incident wavelengths. The white dashed line indicates the focal plane at 49 μm . **c**, Measured focal length. **d**, Operation efficiency. **e**, Full width at half maximum (FWHM) of light profile. Error bars are the standard deviation of the measured efficiencies from different metalenses of the achromatic metalens array. The intensity pattern after the metalens is recorded step by step along the propagation direction with a step of 1 μm . The efficiency is defined as the ratio of the power of the circularly polarized light to that of the incident light with the opposite handedness. All points and error bars represent the mean and standard deviation of experiments results.



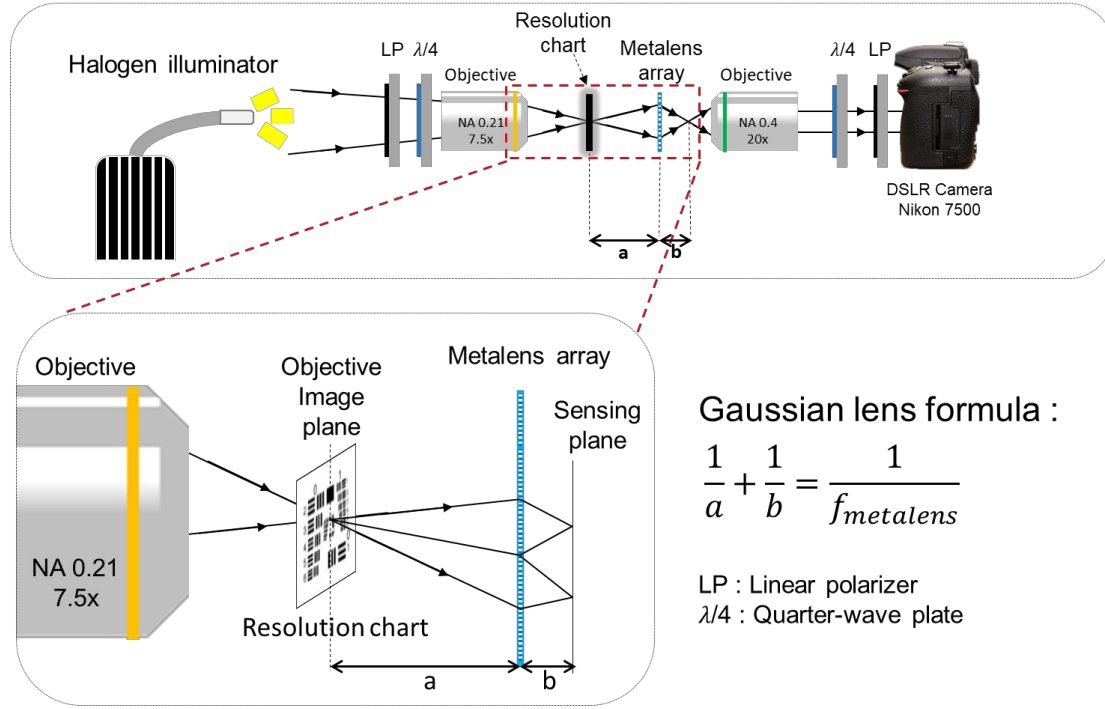
Supplementary Fig. 4: The MTF curves of the theoretical diffraction-limit and achromatic metalens at three wavelengths (400 nm, 540 nm and 660 nm). The MTF curves are calculated by using the Fourier transform of the point spread function (PSF).



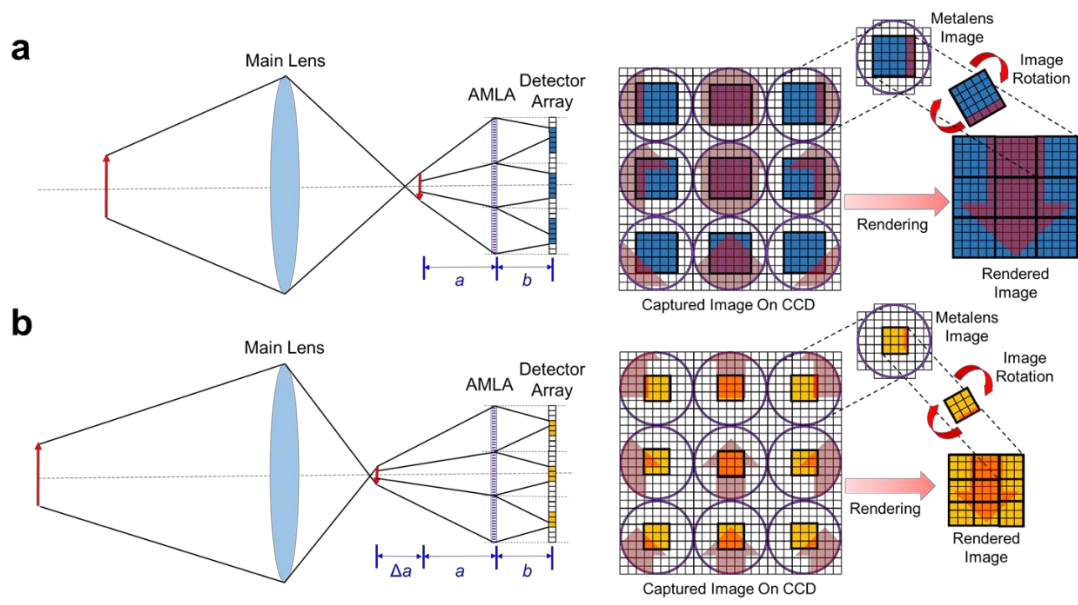
Supplementary Fig. 5: Schematic layout of focused light field microscopy with achromatic metalens array. A halogen lamp is used as the broadband light source to illuminate the target object. Circularly polarized light is generated by a linear polarizer and a quarter-wave plate. An objective (7.5 \times magnification, NA = 0.21, Mitutoyo) is used to collect the light on the achromatic metalens array, and another objective (20 \times magnification, NA = 0.4, Mitutoyo) is used to form the reimaging image from the achromatic metalens array on the camera (Nikon 7500). The position of the metalens array for the focused light field follows the Gaussian lens formula: $1/a + 1/b = 1/f$, where f is the focal length of a single metalens, and a and b are the distance from the main lens image plane to the metalens array and the distance from the metalens array to the reimaging plane, respectively.



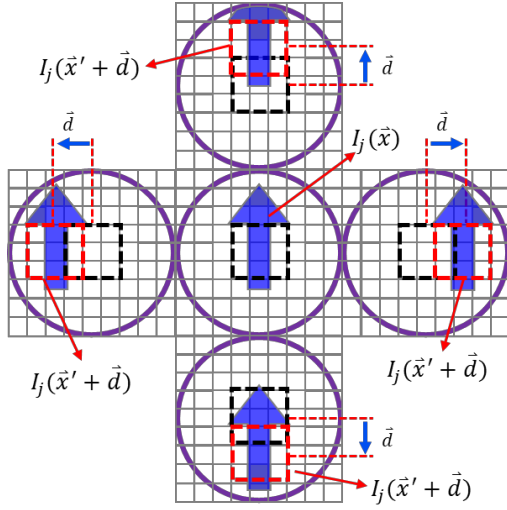
Supplementary Fig. 6: Schematic layout of focused light field microscopy with achromatic metalens array for the scene showing Earth, a rocket and Saturn. A white light LED source is used as the broadband light source to illuminate the target object. The rocket is set as the linear moving target with constant moving velocity of 1 cm/s and mounted on a linear stage (ODL220/M, Thorlab) with a resolution of 2 μm .



Supplementary Fig. 7: Schematic layout of focused light field microscopy with achromatic metalens array for the lateral resolution test. A 1951 USAF resolution test chart is placed in front of the achromatic metalens array. The halogen lamp used as the broadband incoherent light source is collimated by an objective (7.5 \times magnification, NA = 0.21, Mitutoyo) to illuminate the resolution test chart. The feature sizes of the grating structures on the resolution chart are from 2000 μm to 0.55 μm . The image of the resolution chart is projected to the achromatic metalens array. Another objective (20 \times magnification, NA = 0.4, Mitutoyo) is used to relay the image information passing through the achromatic metalens array to the camera (Nikon 7500).



Supplementary Fig. 8: The rendering algorithm for focused light field imaging with different patch sizes for different depths of focus. a, Near object. b, Distant object.

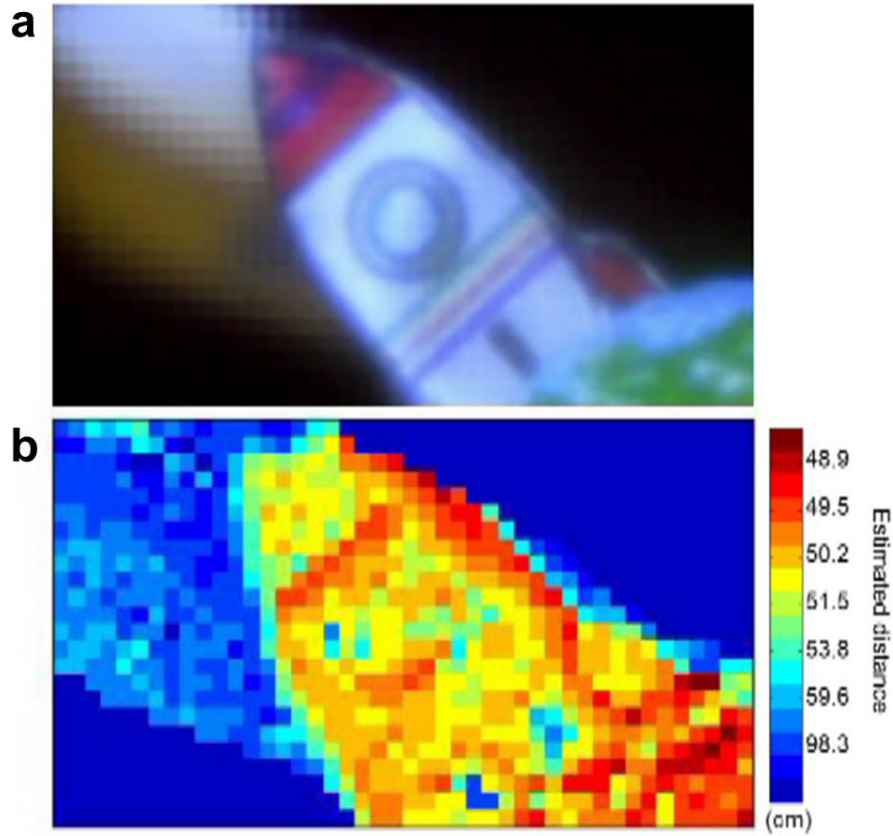


$$(i). D(\vec{d}) = \sum_{j=R,G,B} (I_j(\vec{x}' + \vec{d}) - I_j(\vec{x}))^2$$

$$(ii). D(\vec{d}_{min}) = \text{Min}(D(\vec{d}))$$

$$(iii). \text{disparity} = |\vec{d}_{min}|$$

Supplementary Fig. 9: Depth estimation algorithm. The depth information is obtained from the disparities (or cross correlations) between neighboring subimages.



Supplementary Video 1: A real-time depth map video of the scene of the combination of Earth, a rocket and Saturn. The rocket is moving towards Saturn. **a**, The rendered video refocusing on the rocket. **b**, Corresponding depth map video of **a**.

References

1. Barker Jr, A. & Ilegems, M. Infrared lattice vibrations and free-electron dispersion in GaN. *Phys. Rev. B* **7**, 743 (1973).